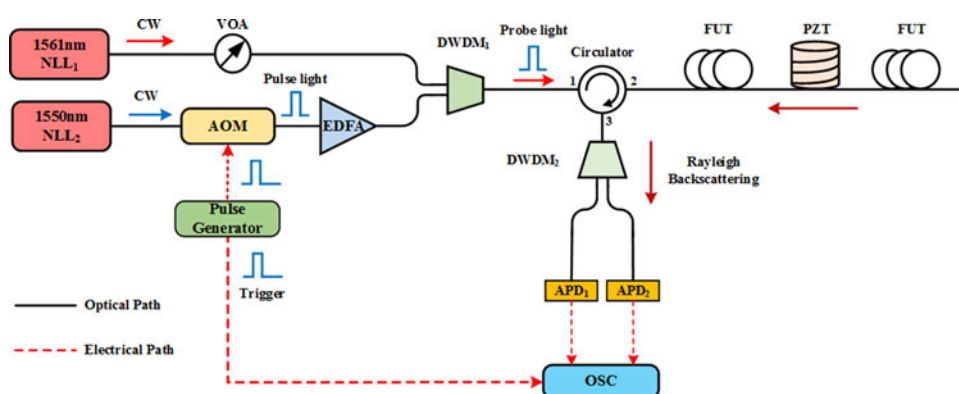


# A Broadband Distributed Vibration Sensing System Assisted by a Distributed Feedback Interferometer

Volume 10, Number 1, February 2018

Yuanyuan Shan  
Jiayun Dong  
Jie Zeng  
Siyi Fu  
Yinsen Cai  
Yixin Zhang  
Xuping Zhang



DOI: 10.1109/JPHOT.2017.2776919  
1943-0655 © 2017 IEEE

# A Broadband Distributed Vibration Sensing System Assisted by a Distributed Feedback Interferometer

Yuanyuan Shan<sup>1</sup>,<sup>1</sup> Jiayun Dong,<sup>1</sup> Jie Zeng,<sup>2</sup> Siyi Fu,<sup>1</sup> Yinsen Cai,<sup>1</sup>  
Yixin Zhang,<sup>1,3</sup> and Xuping Zhang<sup>1,3</sup>

<sup>1</sup>Institute of Optical Communication Engineering, Nanjing University, Nanjing 210093, China

<sup>2</sup>State Key Laboratory of Mechanics and Control of Mechanical Structures, Nanjing University of Aeronautics and Astronautics, Nanjing 210016, China

<sup>3</sup>Key Laboratory of Modern Acoustics, Nanjing University, Nanjing 210093, China

DOI:10.1109/JPHOT.2017.2776919

1943-0655 © 2017 IEEE. Translations and content mining are permitted for academic research only.

Personal use is also permitted, but republication/redistribution requires IEEE permission.

See [http://www.ieee.org/publications\\_standards/publications/rights/index.html](http://www.ieee.org/publications_standards/publications/rights/index.html) for more information.

Manuscript received September 28, 2017; revised November 13, 2017; accepted November 20, 2017. Date of publication November 23, 2017; date of current version February 1, 2018. This work was supported by the National Natural Science Foundation of China under Grant 61405090 and Grant 61627816. Corresponding authors: Y. Zhang and X. Zhang (e-mail: zyixin@nju.edu.cn; xpzhang@nju.edu.cn).

**Abstract:** A distributed vibration-sensing system based on phase-sensitive optical time-domain reflectometry ( $\Phi$ -OTDR) and distributed feedback interferometer (DFI) with broadband frequency response and high spatial resolution has been proposed and demonstrated. A couple of narrow line-width lasers with different wavelengths were used to form the light source, which were consistent with two channels of dense wavelength division multiplexer. Both functions of  $\Phi$ -OTDR and DFI could work synchronously without influence between each other. The characteristic of broadband frequency disturbance event could be fully captured and identified by the DFI, while the corresponding location could be determined by the  $\Phi$ -OTDR scheme. Unlike ordinary interferometer, the proposed DFI scheme could make single-end monitoring without the installation of extra accessories. Furthermore, broadband frequency response range and precise locating of the disturbance event could be achieved at the same time. Experimental results have shown that spatial resolution of 10 m and frequency response up to 1 MHz have been obtained over 2.16-km-sensing fiber, which have proved the validity of the proposed method.

**Index Terms:** Distributed vibration sensing system, phase-sensitive OTDR, interferometry, vibration measurement, broadband frequency response.

## 1. Introduction

Distributed vibration sensing (DVS) system has been studied extensively and applied in numerous fields, owing to its advantages of high sensitivity and long-distance monitoring ability [1]–[4]. In the large-scale structure health monitoring, both the spatial and frequency features of the disturbance events are required [5], which could be used to make early warning before serious damage actually happens. Commonly, disturbance events such as crack of bridges and leakage of high-pressure pipelines would generate weak but noteworthy high frequency vibration, whose frequency range extends to MHz level [4], [6]. Therefore, distributed optical fiber vibration sensors with high spatial resolution and broadband frequency response are urgently needed.

Up to the present, the methods of distributed optical fiber vibration measurement mainly include optical fiber interferometer sensors and optical time domain reflectometry sensors [4]. Optical fiber interferometer sensors include Mach-Zehnder interferometer (MZI), Sagnac interferometer, and Michelson interferometer [7]–[9], which commonly have wide frequency response range of MHz. The detectable frequency range of interferometer sensors is only limited by the bandwidth of the optoelectronic receiver. However, most existing interferometer sensors need a loop structure or a reflector at the rear end of the sensing fiber, which is inconvenient or even impossible to achieve in most practical situations. In order to obtain the location information of disturbance event, two kinds of interferometers are often integrated together, leading to complicated signal processing, relatively low spatial resolution or measurement blind zone [8], [10].

Recently, vibration measurement based on phase-sensitive optical time domain reflectometry ( $\Phi$ -OTDR) has become more popular for its reasonable spatial resolution, multipoint detection capacity and single-end structure. If a disturbance event is applied on the fiber, the shape of the Rayleigh back-scattering (RBS) trace will change at corresponding position. By observing the variation of RBS trace, the location and frequency of the disturbance event can be obtained. However, for preventing backscattered light from different probe pulse overlapping, the repetition period  $T$  of the probe pulse should be larger than the round-trip time that one pulse travels through the sensing optical fiber. The maximum detectable frequency would be limited to  $1/2T$  according to the Nyquist sampling theorem. For 1 km sensing fiber, without any multiplexing technique, the maximum detectable frequency would be 50 kHz for a traditional  $\Phi$ -OTDR. Therefore, there exists a trade-off between the sensing range and detectable frequency range, which would limit the measurement of broadband frequency disturbance events.

Many efforts have been made to extend the frequency response range of  $\Phi$ -OTDR system. A multi-pulse  $\Phi$ -OTDR employing frequency division multiplexing has been demonstrated [11], which can realize 20 kHz frequency response over 10 km sensing range. Detections of high vibration frequency up to 0.6 MHz with time-division multiplexing has been proposed, which successfully gained 680 m sensing fiber length with 1 m spatial resolution [12].  $\Phi$ -OTDR combined with MZI based on frequency division multiplexing has been put forward with 40 kHz frequency response [13]. A MZI and  $\Phi$ -OTDR merging scheme using modulated time-difference pulses has been reported [4], [5], which could reach up to 6.3 MHz frequency response [5]. A single-end-access  $\Phi$ -OTDR merged MZI structure has also been proposed, which can obtain 1.2 MHz frequency response [14]. However, all these hybrid structures were two-end structure or needed a “frequency shift mirror” at the rear end of the fiber, which would be inconvenient in practical applications.

This paper discusses a distributed feedback interferometer (DFI) structure based on the scattering points within the optical fiber, which could realize broadband frequency response range. Assisted by DFI structure, the detection bandwidth of proposed  $\Phi$ -OTDR system would be enhanced. High spatial resolution, broadband frequency response and the capacity for single end sensing could be achieved in one system.

## 2. Principle of High Frequency Vibration Measurement

The continuous wave (CW) light and probe pulse light are injected into the sensing fiber at the same time. The RBS light generated by the CW light can be written as:

$$E_{CW}(t) = \sum_{k=1}^M E_{ck} \cos(2\pi f_1 t + \varphi_k) \quad (1)$$

Where,  $E_{ck}$  is the complex amplitude of RBS light produced by CW light.  $f_1$  is the center frequency of the  $NLL_1$ .  $M$  is the total number of scattering points within an entire sensing fiber.  $\varphi_k$  is the initial phase of the  $k_{th}$  point. Then, the interference between the RBS light waves can be described as:

$$i_{CW}(t) \propto E_{CW}^2(t) = \sum_{k=1}^M E_{ck}^2 + 2 \sum_{k \neq j} E_{ck} E_{cj} \cos(\varphi(t) + \Delta\varphi_{k,j}) \quad (2)$$

Where,  $\varphi(t)$  is the vibration-induced phase change,  $\Delta\varphi_{k,j}$  is the initial phase difference between two scattering points. The interference signal is sampled in time domain, and then the characteristics in frequency domain are obtained by fast Fourier transform (FFT).

Meanwhile, for each individual probe pulse light, the RBS lights within a pulse can be expressed as:

$$E_p(t) = \sum_{k=1}^N E_{pk} \cos(2\pi(f_2 + \Delta f)t + \varphi_k) \quad (3)$$

Where,  $E_{pk}$  is the complex amplitude of backscattering light of pulse light.  $f_2$  is the center frequency of the NLL<sub>2</sub>.  $\Delta f$  is the frequency shift generated by an acoustic-optic modulator (AOM).  $\varphi_k$  is the initial phase of  $k_{th}$  point, and  $N$  is the total number of scattering points within a pulse. Then the received photocurrent is given by:

$$i_p(t) \propto E_p^2(t) = \sum_{k=1}^N E_{pk}^2 + 2 \sum_{k \neq j} E_{pk} E_{pj} \cos(\varphi(t) + \Delta\varphi_{k,j}) \quad (4)$$

To enhance the signal-to-noise ratio (SNR), we adopt the mean-variance method to locate the vibration. This method essentially measures the amplitude fluctuation of the Rayleigh backscattering signal within a certain time window. The mean-variance method can be written as:

$$S = \frac{1}{K} \sum_1^K \left[ i_p(t) - \frac{1}{K} \sum_1^K i_p(t) \right]^2 \quad (5)$$

Where,  $K$  is the number of consecutive traces sampled within the time window. The DFI structure can obtain the true frequency spectrum of high-frequency vibration without aliasing in the frequency domain, but the interference signal does not carry the location information. When multi-point vibrations occur at the same time, the obtained spectrum will exhibit multiple peaks and the frequency corresponding to each vibration cannot be differentiated. Therefore, multi-point disturbance events cannot be distinguished only by DFI structure. Meanwhile, the aliasing spectrum at the disturbance position can be obtained by  $\Phi$ -OTDR system with under-sampling rate. Thus, by mapping the aliasing spectrum to the true spectrum, the position information and frequency response of multi-point vibrations can be measured precisely by this sensing system. Assuming the disturbance event is of single frequency, there is a certain mathematical relation between the aliasing and true spectrum based on the Nyquist sample theorem, which can be written as [13]:

$$f_{\text{aliasing}} = |f_{\text{true}} - mf_s| \quad (m \in \mathbb{Z}, |f_{\text{true}} - mf_s| < f_s/2) \quad (6)$$

Where  $f_{\text{aliasing}}$  is the aliasing frequency obtained by  $\Phi$ -OTDR system with under-sampling rate,  $f_{\text{true}}$  is the true frequency obtained by DFI structure with over-sampling rate.  $f_s$  is the repetition frequency of the pulse light.  $m$  is an integer, which makes the high frequency component move to the frequency range from  $-f_s/2$  to  $f_s/2$ . For example, assuming that the true frequency of target signal is 200 kHz. In the over-sampling rate case, the signal is sampled with the sample rate of 1 MSa/s. In the under-sampling rate case, the sample rate is 60 kSa/s. According to Eq. (6), the  $f_{\text{aliasing}}$  of the target signal would be 20 kHz. The simulation results are shown in Fig. 1.

### 3. Experimental Setup

Fig. 2 shows the experimental configuration of the proposed system. The center wavelengths of NLL (RIO Orion TM Laser module) were set as 1550.12 nm and 1561.42 nm, with the output power of 8dBm and linewidth of 3.7 kHz, respectively. The CW of NLL<sub>1</sub> was first adjusted by the variable optical attenuator (VOA) and then injected into the dense wavelength division multiplexer (DWDM<sub>1</sub>). The CW light of NLL<sub>2</sub> was shaped by an AOM into narrow probe pulse light with frequency shift of 150 MHz. The repetition period and pulse width of the pulse light were 37  $\mu$ s and 100 ns, corresponding to the highest detectable frequency of 13.5 kHz and spatial resolution of 10 m,

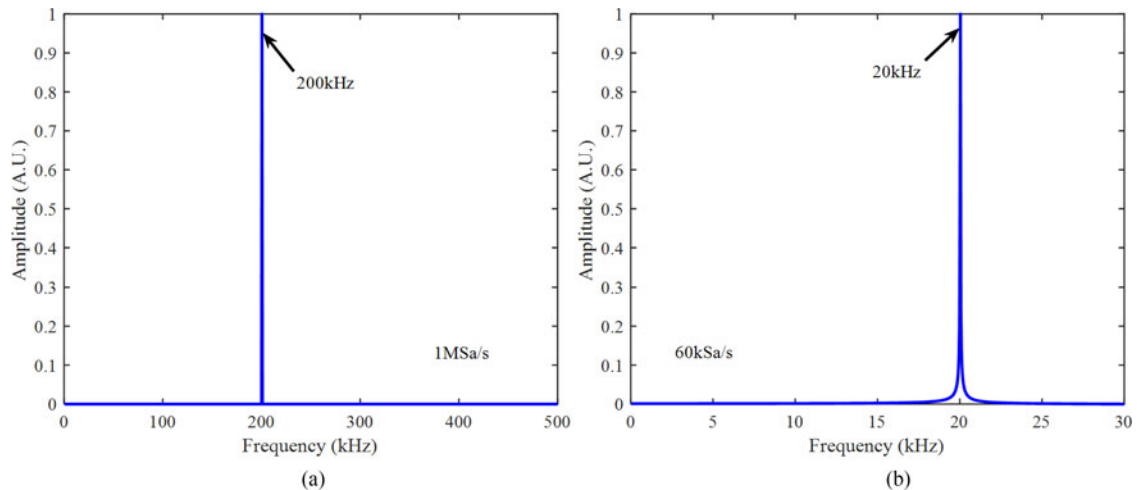


Fig. 1. The simulated results of 200 kHz. (a) The true spectrum in over-sampling rate. (b) The aliasing spectrum in under-sampling rate.

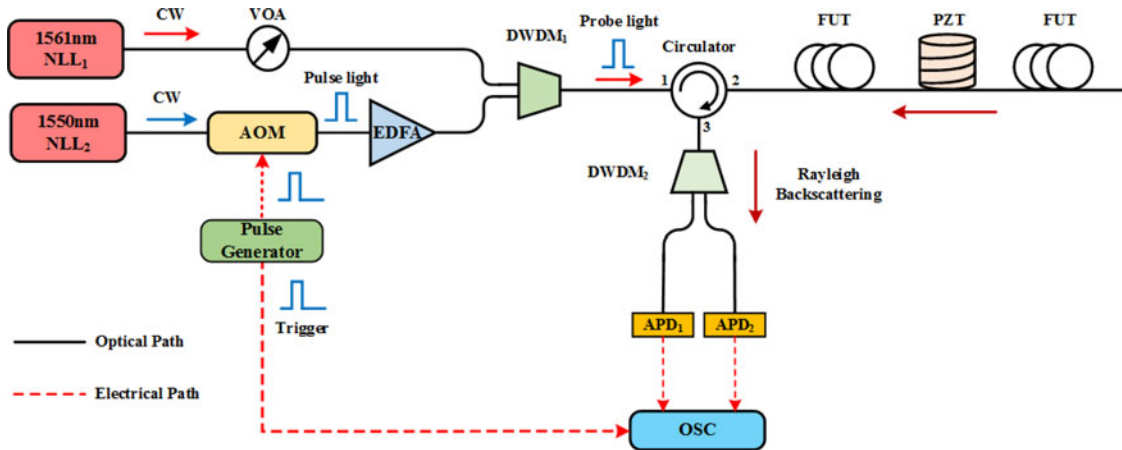


Fig. 2. Experimental setup of proposed system. NLL<sub>1,2</sub>: narrow linewidth laser; CW: continuous wave; VOA: variable optical attenuator; AOM: acoustic-optic modulator; EDFA: erbium-doped fiber amplifier; DWDM<sub>1,2</sub>: dense wavelength division multiplexer; FUT: fiber under test; APD<sub>1,2</sub>: avalanche photodiode; OSC: oscilloscope.

respectively. Then the modulated pulse was amplified by an erbium-doped fiber amplifier (EDFA). The pulse light combined with the CW light were injected into sensing fiber through circulator simultaneously. Due to the narrow linewidth of NLL<sub>1</sub>, the corresponding coherent length of the light was no less than 80 km, which was much longer than the sensing fiber length of 2.16 km. Therefore, all the scattering points along the optical fiber could be regarded as distributed reflectors of an interferometer. The RBS lights of the CW light could interfere with each other within the entire optical sensing fiber. At last, a distributed feedback interferometer with single-end was achieved. Then, the RBS lights of the CW light and probe pulse light went through the same circulator and separated by DWDM<sub>2</sub>. The signals were detected by avalanche photodiodes (APD) with the bandwidth of 200 MHz, respectively. Then, the  $\Phi$ -OTDR traces and interference signals were recorded by oscilloscopes (OSC) simultaneously, which was in synchronization with AOM by the pulse generator.

## 4. Experimental Results and Discussions

### 4.1. The Results of Single Vibration

When the frequency of vibration exceeds 13.5 kHz, due to the 27 kHz sampling rate of  $\Phi$ -OTDR system, the spectrum measured by  $\Phi$ -OTDR will be aliasing. The sampling rate of DFI structure was set as 5 MHz which was high enough to obtain the true spectrum of high frequency vibration. So, assisted by the DFI structure, the frequency response range of  $\Phi$ -OTDR system could be extended. In this experiment, a PZT was used as the vibration source, whose maximum vibration frequency was 1 MHz. The PZT twined with 10 m fiber was set at 1.533 km. The frequencies of the waveforms applied to the PZT were 0.1 MHz, 0.3 MHz, 0.5 MHz, 0.7 MHz and 1 MHz. The 2000 consecutive  $\Phi$ -OTDR traces and 74 ms interference signal were recorded simultaneously. The total recording time was 74 ms, respectively. After signal processing, the FFT results of the signals obtained by DFI structure were illustrated in Fig. 3(a). Compared with the far end white noise floor, the power spectrum showed clearly visible peaks in all applied frequencies with high SNRs, which were 38.80 dB, 34.34 dB, 32.68 dB, 30.99 dB and 30.59 dB, respectively. It is obvious that the peak value decreased with the increasing of the frequency. This corresponds to the fact that, as the frequency is increased, the electric energy to mechanical energy transducing efficiency of PZT is decreased. Thus, under the same driving voltage, the fiber displacement caused by PZT would be reduced. The vibration position of each frequency could also be obtained by  $\Phi$ -OTDR system and distinguished obviously, as shown in Fig. 3(b). In this setup, the center of PZT stretching region was located at 1.533 km. According to Fig. 3(b), the obtained positions were distributed within the range between 1.535 km to 1.53 km. That means the uncertainty of the locating process for the proposed system was only 5 m under the spatial resolution of 10 m.

### 4.2. The Results of Dual Vibrations

To demonstrate the capability of multi-point vibration sensing, dual vibration events with frequencies of 5 kHz and 20 kHz were applied to the sensing fiber at the position of 0.52 km and 1.533 km, respectively. Two peaks appeared at 0.52 km and 1.534 km clearly, where the front and rear peak were presented as point A and point B, given in Fig. 4(a). From Fig. 4(b) and (c), it can be observed that the spectrum with the peak of 5 kHz and 7 kHz were detected at point A and point B (through  $\Phi$ -OTDR traces), respectively. Meanwhile, the true spectrum of the dual vibrations measured by DFI structure with the peak of 5 kHz and 20 kHz was given in Fig. 4(d), which were agreed with the applied frequencies. In this setup, the sample rate of  $\Phi$ -OTDR was 27 kHz (corresponding to the pulse repetition period of 37  $\mu$ s). According to Eq. (6), the peak in Fig. 4(c) equaled to the aliasing frequency of 7 kHz ( $f_{\text{aliasing}} = |27 - 20|$  kHz). Therefore, the vibration with frequency of 20 kHz occurred at point B.

### 4.3. The Results of Knocking Events

In order to further verify the capability of the proposed system for capturing broadband signals, knocking-event was considered as disturbance source, assuming the frequency spectrum can cover the band from few Hz to several hundreds of kHz. 25 loops of bare single mode fiber with 13 cm diameter were glued a thin aluminum board with 1 cm thickness, as given in Fig. 5. The total length of fiber glued on the board was 10.2 m, which was located at the position of 543 m. An iron-hammer and a rubber-hammer were used to knock the aluminum board, respectively.

In this experiment, the repetition rate of modulated pulse in  $\Phi$ -OTDR and the sampling rate of DFI were set as 1 kHz and 5 MHz, respectively. The 2000 consecutive  $\Phi$ -OTDR traces and 2 s interference signals were recorded simultaneously. So, the total recording time was 2 s, respectively. To get the characteristics of the spectrum over time, the short-time Fourier transform (STFT) was used to process the recorded signals. The window interval of STFT was set as 0.2 s. Fig. 6 showed the position information and aliasing spectrum of knocking event with an iron-hammer obtained by  $\Phi$ -OTDR scheme. The vibration point appeared at 548 m clearly, as given in Fig. 6(a). The spectrum

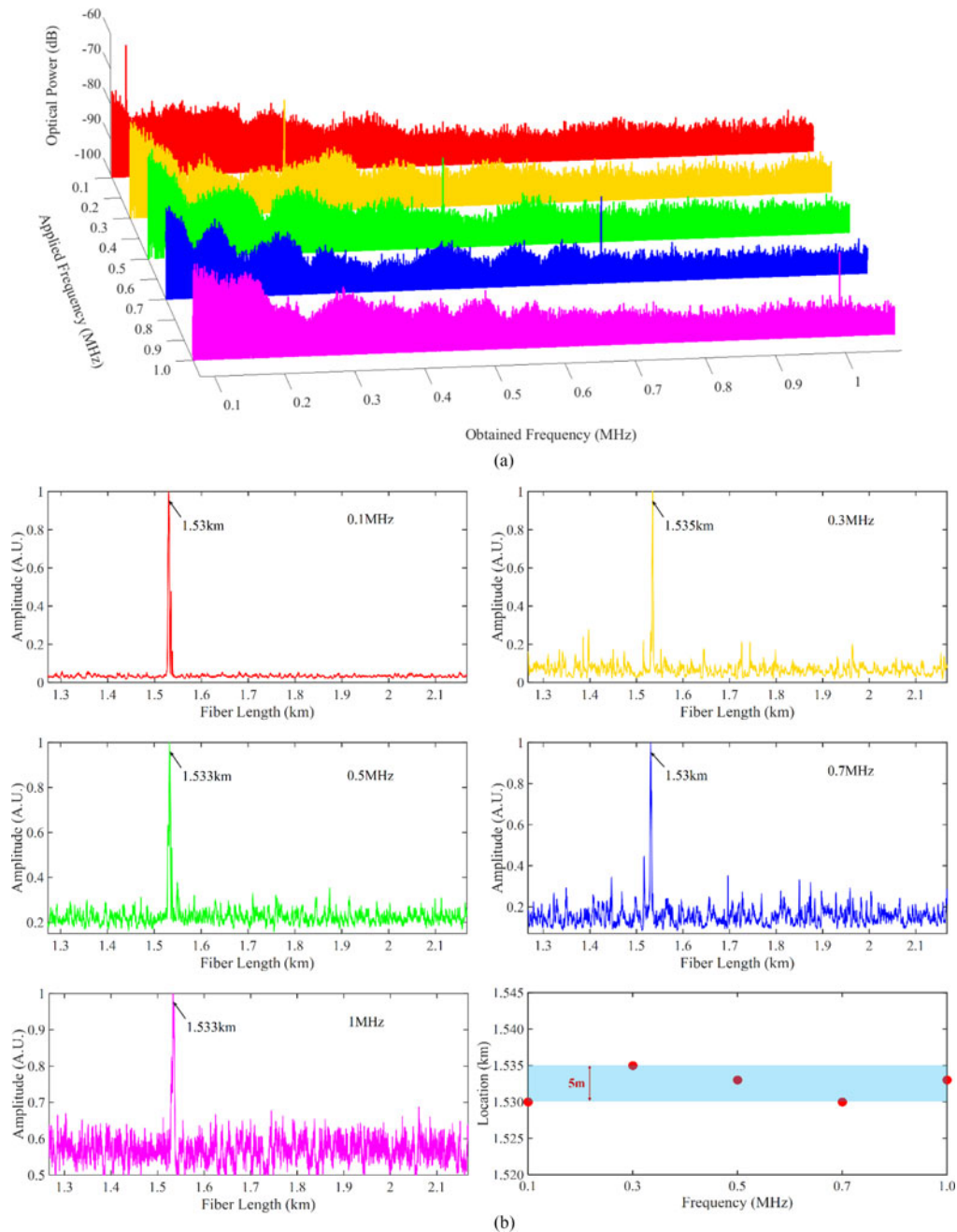


Fig. 3. The experimental results of high frequency vibration. (a) The spectra measured by DFI scheme. (b) The position information measured by  $\Phi$ -OTDR and the uncertainty of location measurement.

of iron-hammer-knocking was illustrated in Fig. 6(b). The intensity of frequency components is mapped into the color of spectrum image. The same signal processing was applied on the rubber-hammer-knocking data. The corresponding position information and aliasing spectrum were shown in Fig. 7(b).

Comparing Figs. 6(b) with 7(b), the displayed frequency components were similar owing to the under-sampling of the  $\Phi$ -OTDR system. The two kinds of knocking events cannot be distinguished only by these characteristics in frequency domain. Therefore, the true spectrum measured by DFI

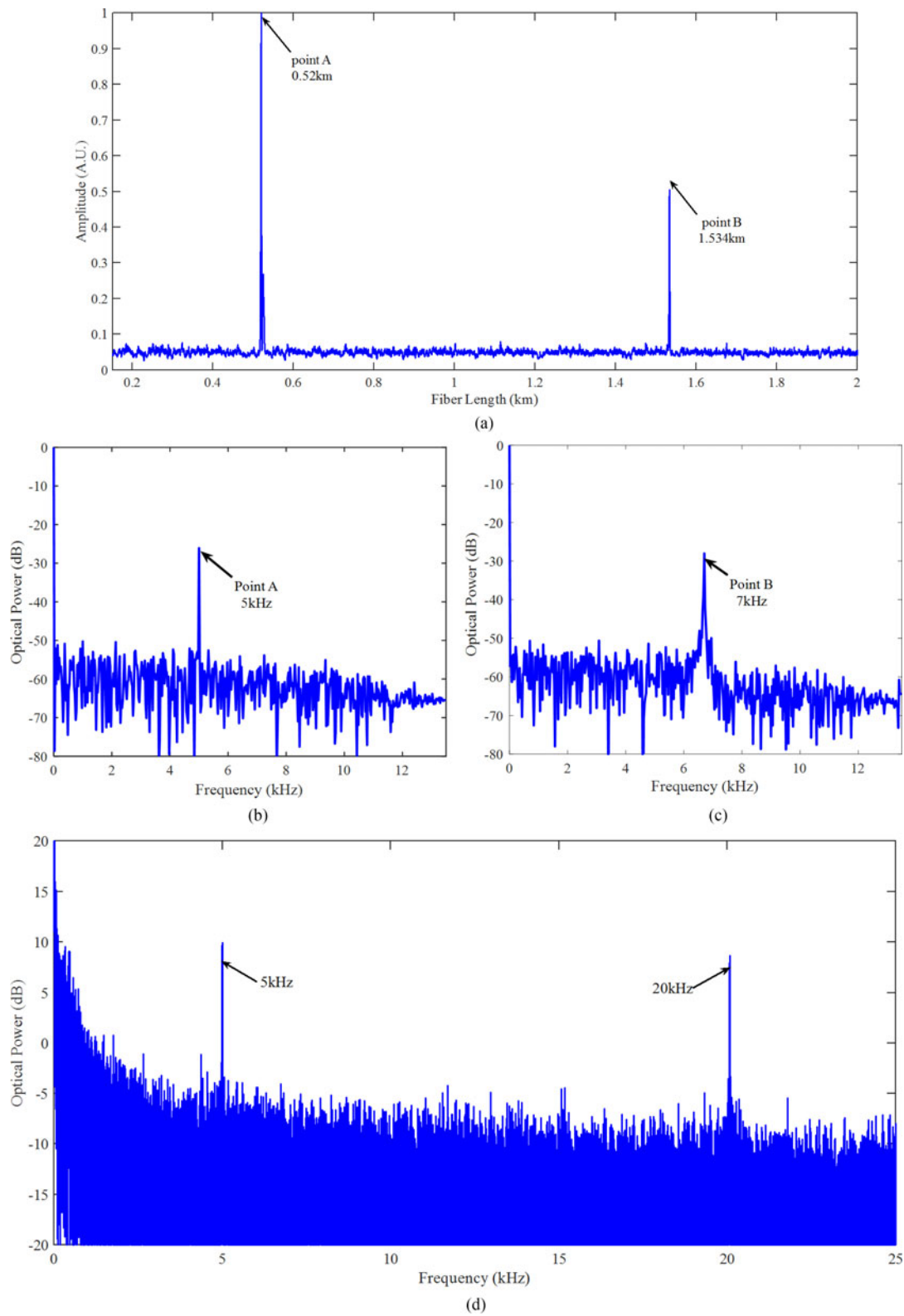


Fig. 4. The position information and frequency spectra obtained by proposed system. (a) The position information of dual vibrations. (b) The spectrum of point A measured by  $\Phi$ -OTDR system. (c) The spectrum of point B measured by  $\Phi$ -OTDR system. (d) The true spectrum measured by DFI structure.



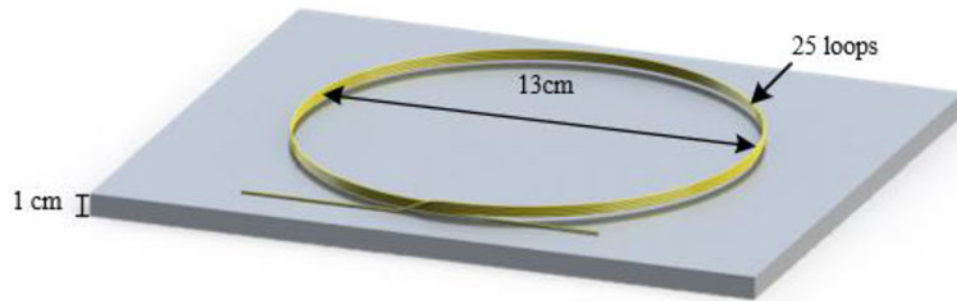


Fig. 5. The schematic diagram of fiber loops.

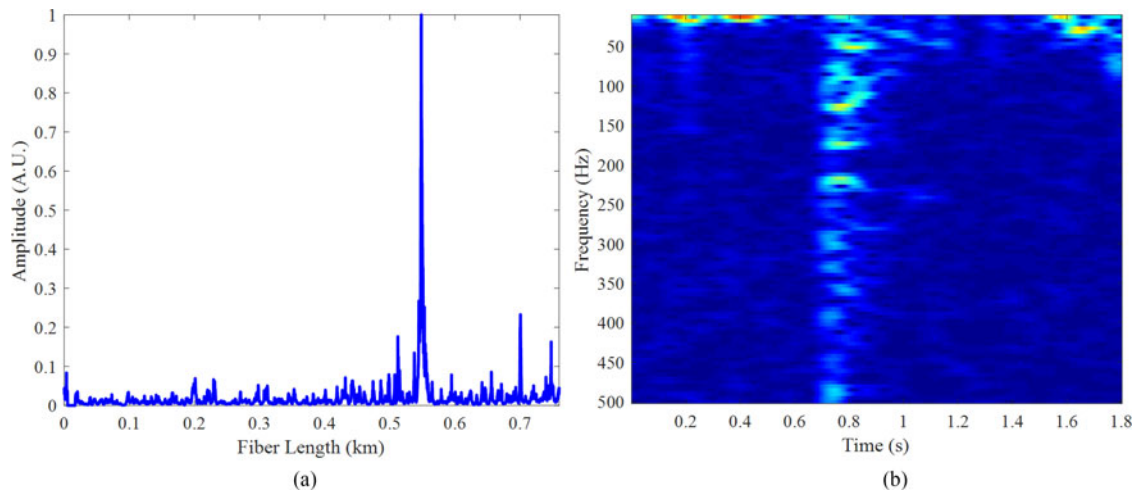


Fig. 6. The position information and spectrum of iron-hammer-knocking measured by  $\Phi$ -OTDR. (a) The location information. (b) The aliasing spectrum of iron-hammer-knocking event.

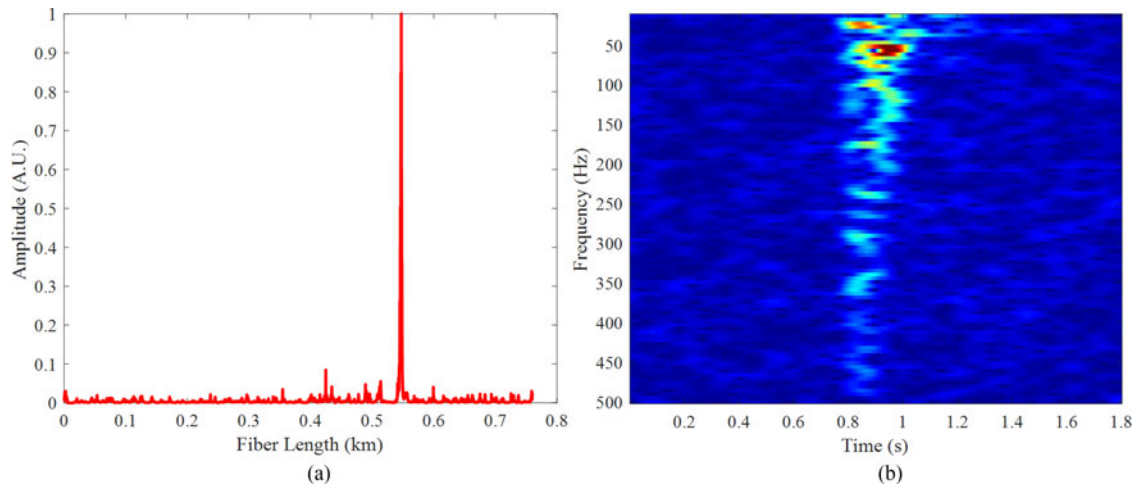


Fig. 7. The position information and spectrum of rubber-hammer-knocking measured by  $\Phi$ -OTDR. (a) The location information. (b) The aliasing spectrum of rubber-hammer-knocking event.

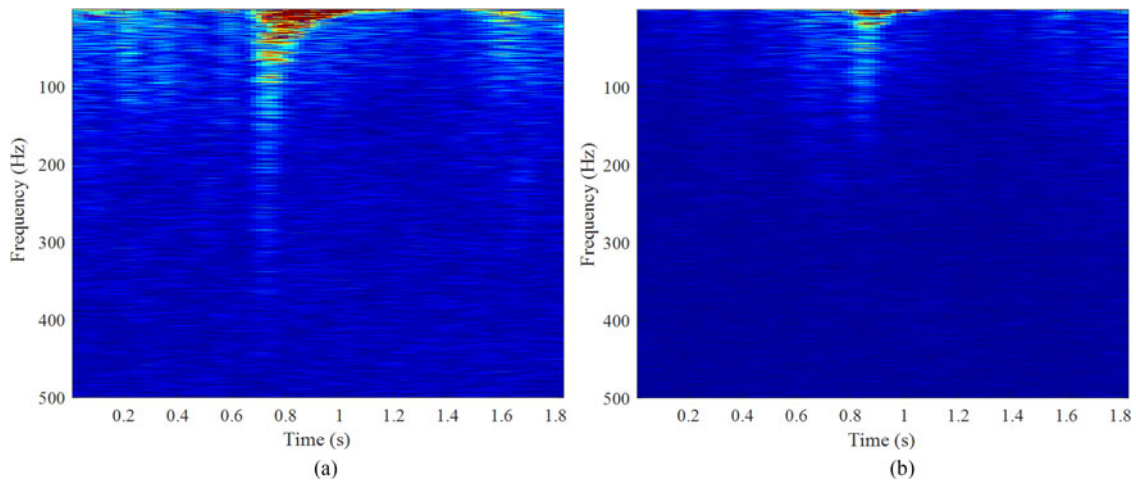


Fig. 8. The true spectra of knocking-events measured by DFI. (a) The spectrum of iron-hammer-knocking. (b) The spectrum of rubber-hammer-knocking.

structure is necessary to assist the  $\Phi$ -OTDR system for distinguishing different events. STFT with window interval of 0.2 s was also applied on the data measured by DFI structure. Owing to the higher sampling rate, the DFI structure could have higher frequency response in the same time interval. The characteristics in frequency domain and duration of vibration caused by knocking were shown in Fig. 8(a), which were obvious different from those of rubber-hammer-knocking as given in Fig. 8(b). The knocking event had a broadband frequency response. And the high frequency components will decay down rapidly. The high frequency components of iron-hammer-knocking were stronger than that of rubber-hammer-knocking, which was almost up to 400 kHz. The duration of vibration caused by iron-hammer-knocking was about 0.5 s, which was also longer than that of rubber-hammer-knocking. The intensity of low frequency in Fig. 8(a) was also larger than that in Fig. 8(b) apparently.

Those differences mentioned above could only be observed from the true spectrum obtained by DFI structure. That is why the DFI structure is introduced to assist  $\Phi$ -OTDR system. The proposed system could achieve high spatial resolution, broadband frequency response and single-end sensing ability. This single-end-access scheme will be more suitable for practical applications.

## 5. Conclusion

In this paper, we have proposed a DVS system based on  $\Phi$ -OTDR system and DFI with broadband frequency response, high spatial resolution and single-end sensing ability. The proposed sensing system has achieved single-end sensing without the installation of extra ancillaries, which would be quite suitable for practical applications. The experiment results have shown that the frequency response of the system could reach up to 1 MHz and no frequency dead zone exist in this sensing system. The SNRs were still above 30.59 dB when different vibrations event applied to the sensing fiber. The measurement uncertainty of vibration event locating was less than 5 m in the spatial resolution of 10 m. And utilizing a DFI structure, the true spectrum of disturbance can be obtained, which gives the sensing system the ability to distinguish different vibration events. Consequently, the proposed system could find important role in these applications where broadband frequency response is needed.

---

## References

- [1] Y. Wang, B. Jin, Y. Wang, D. Wang, X. Liu, and Q. Bai, "Real-time distributed vibration monitoring system using  $\Phi$ -OTDR," *IEEE Sens. J.*, vol. 17, no. 5, pp. 1333–1341, Mar. 2017.
- [2] J. C. Juarez, E. W. Maier, K. N. Choi, and H. F. Taylor, "Distributed fiber-optic intrusion sensor system," *J. Lightw. Technol.*, vol. 23, no. 6, pp. 2081–2087, Jun. 2005.
- [3] J. C. Juarez and H. F. Taylor, "Field test of a distributed fiber-optic intrusion sensor system for long perimeters," *Appl. Opt.*, vol. 46, pp. 1968–1971, 2007.
- [4] Q. He, T. Zhu, X. Xiao, and X. Bao, "Modulated pulses based distributed vibration sensing with high frequency response and spatial resolution," *Opt. Exp.*, vol. 21, pp. 2953–2963, 2013.
- [5] Q. He, T. Zhu, X. Xiao, B. Zhang, D. Diao, and X. Bao, "All fiber distributed vibration sensing using modulated time-difference pulses," *IEEE Photon. Technol. Lett.*, vol. 25, no. 20, pp. 1955–1957, Oct. 2013.
- [6] Y. Lu, T. Zhu, X. Bao, and L. Chen, "Vibration monitoring with high frequency response based on coherent phase-sensitive OTDR method," *Proc. SPIE*, vol. 7753, 2011, Art. no. 77533K.
- [7] C. Zuo, F. Liu, H. Guo, J. Wu, K. Xu, and X. Hong, "Dual Michelson interferometers for distributed vibration detection," *Appl. Opt.*, vol. 50, pp. 4333–4338, 2011.
- [8] C. Ma *et al.*, "Long-range distributed fiber vibration sensor using an asymmetric dual Mach–Zehnder interferometers," *J. Lightw. Technol.*, vol. 34, no. 9, pp. 2235–2239, May 2016.
- [9] K. Wada, H. Narui, D. Yamamoto, T. Matsuyama, and H. Horinaka, "Balanced polarization maintaining fiber Sagnac interferometer vibration sensor," *Opt. Exp.*, vol. 19, pp. 21467–21474, 2011.
- [10] Q. Chen *et al.*, "A distributed fiber vibration sensor utilizing dispersion induced walk-off effect in a unidirectional Mach-Zehnder interferometer," *Opt. Exp.*, vol. 22, pp. 2167–2173, 2014.
- [11] Z. Pan, Z. Wang, H. Cai, R. Qu, and Z. Fang, "High sampling rate multi-pulse phase-sensitive OTDR employing frequency division multiplexing," *Proc. SPIE*, vol. 9157, 2014, Art. no. 91576X.
- [12] Z. Qin, L. Chen, and X. Bao, "Distributed vibration/acoustic sensing with high frequency response and spatial resolution based on time-division multiplexing," *Opt. Commun.*, vol. 331, pp. 287–290, 2014.
- [13] B. Luo *et al.*, "Multiple vibrations measurement using phase-sensitive OTDR merged with Mach-Zehnder interferometer based on frequency division multiplexing," *Opt. Exp.*, vol. 24, pp. 4842–4855, 2016.
- [14] Y. Zhang, L. Xia, C. Cao, Z. Sun, Y. Li, and X. Zhang, "A hybrid single-end-access MZI and  $\Phi$ -OTDR vibration sensing system with high frequency response," *Opt. Commun.*, vol. 382, pp. 176–181, 2017.